Climate Dynamics (2000) 16:303–317

R. S. Nanjundiah

Impact of the moisture transport formulation on the simulated tropical rainfall in a general circulation model

Received: 7 August 1998 / Accepted: 15 October 1999

Abstract The impact of numerical modeling of moisture transport on the simulation of the seasonal mean pattern of precipitation in the tropics is studied. The NCAR CCM2 with spectral and semi-Lagrangian moisture transport has been used for this purpose. The differences in the numerical modeling of moisture transport are found to have a significant impact on the simulation of the seasonal mean patterns. The major differences while using the spectral method (vis-a-vis the semi-Lagrangian method) are (1) a decrease in rainfall over the Indian monsoon region, (2) a decrease in rainfall over the west Pacific region and (3) an increase in rainfall over the central and east Pacific regions. There are substantial differences in the amount of precipitable water vapor simulated by the two moisture transport techniques. It is shown that the difference in precipitable water vapor between the two simulations is associated with changes in the vertical moist static stability (VMS) of the atmosphere, and differences in the simulated precipitation patterns.

1 Introduction

Water vapor plays an important role in various atmospheric processes such as energy transfer between surface and the atmosphere through evaporation, and in modulating the radiative balance of the Earth-atmosphere system through greenhouse and cloud-albedo effects. Despite its major role in the climate system, water vapor is one of its most poorly modeled subcomponents. Schemes developed for modeling the dynamical motions of the atmosphere (e.g., winds and temperature) such as the spectral method have been adapted for modeling water vapor. However major differences exist between the distribution of temperature and water vapor. While the winds and temperature vary smoothly over the entire atmosphere, most of the water vapor is contained in the lowest 2–3 km of the atmosphere. Also water vapor varies by several orders of magnitude between the equator and the poles. Hence it is not surprising that the adoption of dynamical modeling techniques such as the spectral method causes the simulation of water vapor to be poor.

The shortcomings of spectral methods for moisture transport have been well documented (Laprise 1988). The major problems associated with spectral transport of water are undershooting and overshooting. Undershooting causes negative values of moisture. Overshooting leads to spurious rainfall (especially in regions of near saturation). Procedures required to remove negative moisture are more than cosmetic in nature and could have significant impact on the simulation of the water vapor itself (Williamson and Rasch 1994). To avoid the shortcomings of the spectral method, alternatives such as the semi-Lagrangian transport (SLT) method has been tried. The semi-Lagrangian method does not conserve a priori, but upon using the fixing method as given in Williamson and Rasch (1994), the conservation is satisfactory. Issues regarding conservation in spectral and semi-Lagrangian methods are extensively discussed in Williamson and Rasch (1994).

Williamson and Rasch (1994) and Rasch and Williamson (1991) have studied the sensitivity of climate simulations to the modeling of moisture transport using the spectral (SPT) and SLT techniques. They have studied its impact on the global and zonal averages and have concluded that modeling of moisture transport can have a significant impact on the simulated global and zonal means of various atmospheric parameters (such as precipitation, precipitable water, winds etc). They also show that SLT improves the model's moisture simulations in terms of the global means (such as the mean precipitation, the mean precipitable water, etc). They, however, have not addressed the particular question of

R. S. Nanjundiah
Centre for Atmospheric & Oceanic Sciences,
Indian Institute of Science, Bangalore 560012, India
E-mail: ravi@caos.iisc.ernet.in

the impact of moisture transport on the circulations in the tropics. This is of particular importance as moisture plays a governing role (through deep convection) in modulating both the major circulation patterns in the tropics in particular the Hadley circulation and the Walker circulation. A very recent work of Codron and Sadourny (submitted 1999) with the LMD model has also highlighted the importance of moisture advection in modeling the Indian summer monsoon.

Hence it is considered necessary to study the impact of moisture transport on the simulation of precipitation in the tropics with particular emphasis on the Asia-Pacific region both during the northern summer (June, July and August, JJA) and the northern winter (December, January, and February, DJF) seasons.

2 The model

We have used the CCM2 at T-42 resolution with 18 levels in the vertical. This gives a resolution of approximately 2.8° in the tropics. This model uses the mass flux parametrization of Hack et al. (1993) for cumulus convection. The model used has an interactive bucket-hydrology to model the surface hydrological processes (field capacity of 15 cm). A detailed description of the model is given Hack et al. (1993). The initial condition is for 1 September, 1987, an analysis dataset obtainable from NCAR's public domain site. Both the runs use climatological SSTs of Shea et al. (1990).

2.1 Simulations

We present results from simulations with the semi-Lagrangian moisture transport (SLT) and the spectral moisture transport (SPT) methods in CCM2. The statistical significance of differences in the tropical/areal means of precipitation is obtained by comparing the 20-year simulation with the SLT method with the five-year spectral simulation. Other comparisons are based on five year averages of the SLT and the SPT simulations. The first ten months of integration are not used in the analysis (to remove spin up effects). Williamson and Rasch (1994) suggest that since the water vapor in the troposphere is replaced on a (approximately) 30-day time scale, a period of about five months is sufficient for the major effects of modifying moisture transport to be seen. We also find that the large-scale features from the first year of integration are very similar to the other years. We consider rejecting the first 10 months of simulations as sufficient to remove spin up effects. It is noteworthy that many other modeling studies have even shorter spin-up periods e.g., Molod et al. (1996) and Chen and Bates (1996) suggest that rejecting first two months of the simulation is sufficient to remove the initial transients.

We present results for the northern summer (July) and northern winter (January) for the tropical/areal means and June, July and August (JJA) and December, January and February (DJF) patterns for other discussions.

3 The simulated mean tropical rainfall

Table 1 shows the mean precipitation during July and January for tropics (30°S–30°N, 0°–360°). The five year model simulated mean tropical precipitation is compared with the observed climatologies of Xie and Arkin (1996) and also with that of Legates and Willmott (1990).

Table 1 Variation of precipitation (mm day^{-1}) for the tropics in the spectral and semi-Lagrangian simulations. (LW) is the Legates and Willmott (1990) climatology of precipitation and (XA), the Xie and Arkin (1996) rainfall dataset

Month	Precipitation		
	SPT	SLT	Obs
July	4.20	4.35	4.06 (LW) 3.87 (XA)
January	4.1	4.40	4.41 (LW) 3.92 (XA)

We notice that the two climatologies differ from each other, probably due to the differing algorithms used in developing these datasets. Legates and Willmott (1990) use station (gage) data over land and ship reports for estimation of oceanic rainfall. Xie and Arkin (1996) use station data and satellite data and merge them together to form a single dataset. Recent work of Arpe et al. (1998) has also found differences amongst observational datasets.

Analyzing the twenty year simulated precipitation with the SLT method we note that the mean for the tropics in July is 4.35 mm day^{-1} with a standard deviation (σ) of 0.06 mm day^{-1}. The minimum value of the tropical July precipitation is 4.22 mm day^{-1} and the maximum value 4.42 mm day^{-1} during the 20 years of simulation with SLT. The mean value for spectral simulation (for a five year simulation) is 4.2 mm day^{-1}.

Interestingly, the difference between the Xie and Arkin (1996) dataset and that of Legates and Willmott (1990) is comparable to the difference in the tropical mean precipitation by the two simulations (Table 1). However upon using randomization tests (Sokal and Rohlf 1981) for the statistical significance of the differences between the two simulations, we find that they are different at the 1% (99% confidence) level.

3.1 Precipitation patterns during northern summer and winter

The precipitation patterns for DJF and JJA for the tropical region are shown in Figs. 1 and 2 respectively. Both the simulations reproduce the large-scale features of precipitation correctly (at least qualitatively) with the Indonesian-west Pacific region having significantly higher rainfall than the eastern Pacific. The SPT simulation shows a pattern with more smaller scale structures and in contrast, the SLT simulation has a smoother spatial structure. Examining the DJF precipitation (Fig. 1) we note that the SPT simulates higher rainfall (vis-a-vis the SLT) over the eastern and central Pacific regions, and lower rainfall over the Indonesian-west Pacific region.

Chen and Bates (1996) have compared the fully semi-Lagrangian GSFC model with its Eulerian (finite difference) version. One of the salient differences between

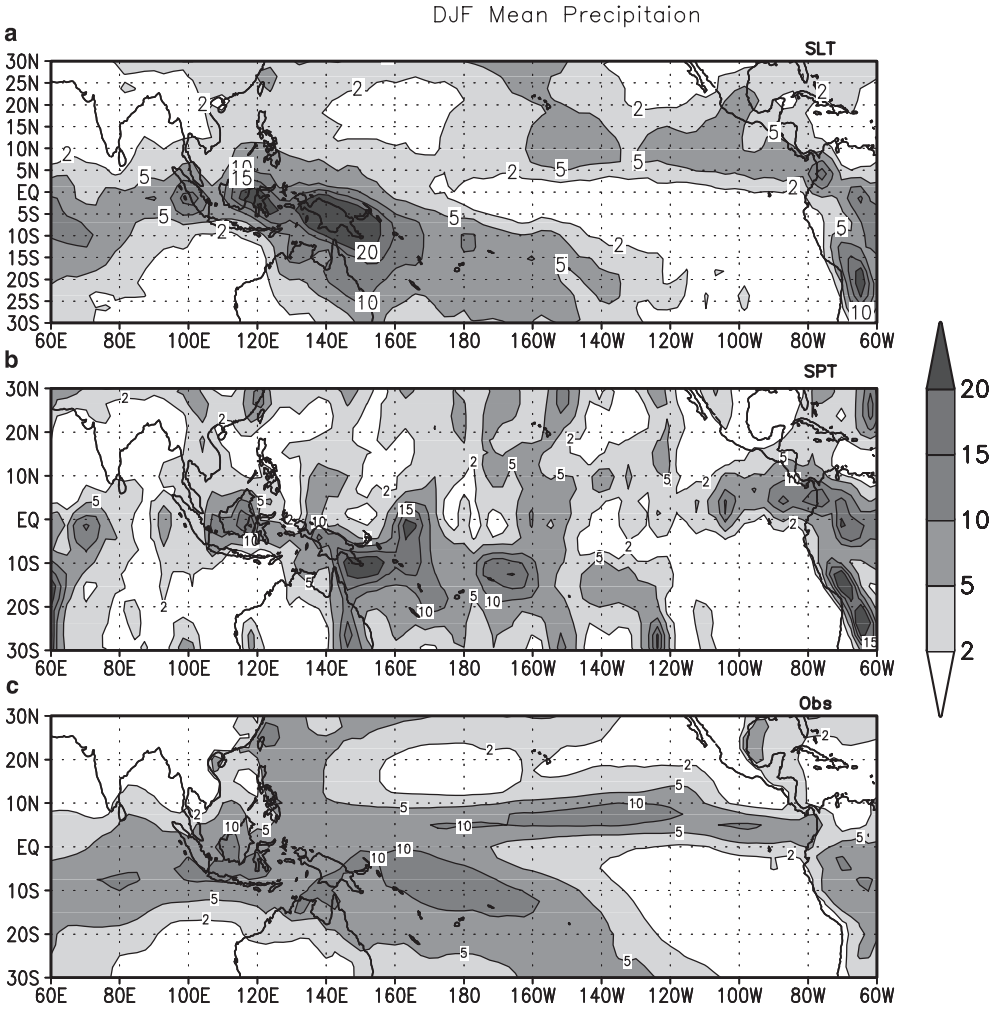

Fig. 1a–c Precipitation (mm day^{-1}) simulated by **a** SLT **b** and SPT and **c** the observed climatology (from Xie and Arkin, 1996) during December, January and February

the simulations by these two versions of the GSFC model is the lower precipitation over the eastern Pacific and overestimation of rainfall over the western Pacific by the semi-Lagrangian version. They speculate the cause of this to be differing responses by the model's dynamics to the cumulus convection scheme. It is noteworthy that the differences in precipitation patterns between Eulerian and semi-Lagrangian GCMs in the study of Chen and Bates (1996) are similar to those found here between the simulations by the same model (CCM2) using the SPT (an Eulerian formulation) and the SLT techniques for moisture transport.

The Indian summer monsoon

The study of Gadgil and Sajani (1998) with the AMIP simulations of the Indian monsoon has shown that modeling of the Indian summer monsoon is still a challenging problem and no model satisfactorily resolves all the observed features. Also most of the water vapor involved in the monsoon precipitation over the South Asian landmass is advected from the surrounding oceanic regions (Hastenrath and Lamb 1980). Hence it is necessary to study the impact of modeling of moisture advection on the Indian summer monsoon. Examining in greater detail the SLT and the SPT simulated precipitation patterns over the Indian region we notice that the spectral simulation shows reduced precipitation over the Indian landmass. The differences between SPT and SLT precipitation simulations over the Indian region are:

1. Reduced rainfall over the peninsular region and the Bay of Bengal
2. Increased rainfall over the equatorial Indian region south of the Indian peninsula

The SLT simulation considerably overestimates the precipitation over the Himalayan/Tibetan region. Over this region (80°E–100°, 25°N–35°) the observed precipitation during July is about 7.8 mm day^{-1}, while the SLT simulates this rainfall as 17 mm day^{-1} and in the spectral simulation this value is closer (but still larger than the climatological mean) at 10.8 mm day^{-1}. The SLT simulation shows a mean rainfall of 7.9 mm day^{-1} over the Indian region with a standard deviation of about 1.6 mm day^{-1}. The spectral transport simulates this rainfall as about 3.0 mm day^{-1} which lies about 3σ beyond the SLT mean.

In making a comparison with the AMIP study for the Indian summer monsoon (Gadgil and Sajani 1998) we note that the SPT scheme's simulation (Fig. 2) is qualitatively similar to that of SUNYA and ECHAM3 (Arpe et al. 1998), while the SLT simulation is similar to the NCAR-CCM2 AMIP simulation (even though the latter was forced with observed SSTs; interestingly Molod et al. 1996, also find that the seasonal mean climatological patterns are largely unaffected by the variation of surface boundary conditions in their simulation study with the GOES-1 GCM). The SUNYA and CCM2 models are derived from the same common source and one of the major significant differences between them being the use of SPT by SUNYA and the use of SLT by CCM2 for moisture transport.

4 The simulated mean tropical precipitable water

Precipitable water is the column integrated value of moisture and the difference in the simulation of this quantity could be related to the modeling of moisture transport. We compare the mean for the 5 years of simulation with the climatological mean values from NCEP-NCAR reanalysis and NVAP dataset (Randel et al. 1996) for precipitable water (Table 2). We note that the total precipitable water averaged over the tropics is higher in the SLT simulation in comparison to the SPT simulation. However, it is noteworthy that between observed datasets themselves there are considerable differences. The July climatological mean for the tropics from the NCEP-NCAR reanalysis is 34.06 kg m^{-2} which is less than the estimate from NVAP (36 kg m^{-2}). The averages for January also show a similar behavior. Mo and Higgins (1996) have also pointed out similar differences in

Table 2 Variation of precipitable water (kg m^{-2}) for the tropics in the spectral and semi-Lagrangian simulations, and observations. NCEP/NCAR reanalysis is shown as (n) while (g) denotes the NVAP dataset values

Month	Precipitable water		
	SPT	SLT	Obs
July	32.82	35.42	34.06 (n) 36.00 (g)
January	30.54	34.59	33.54 (n) 34.77 (g)

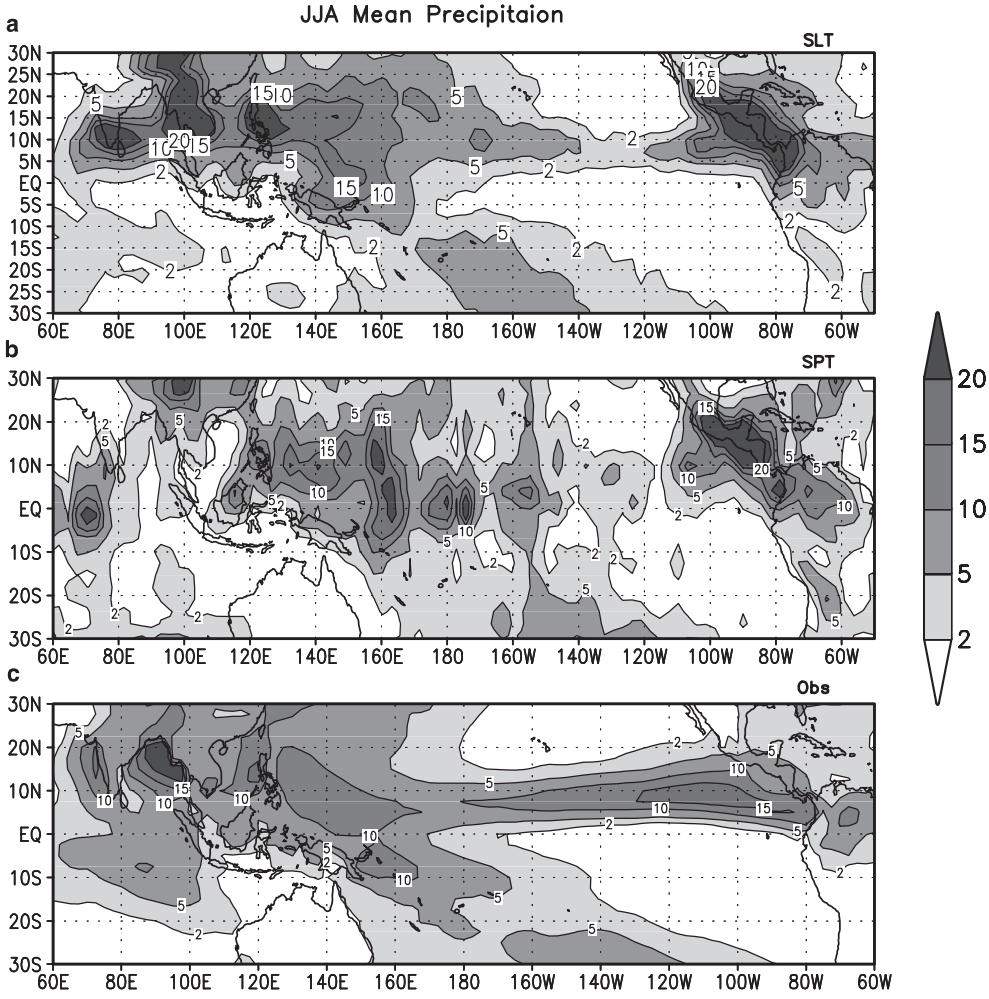

Fig. 2a–c Precipitation (mm day^{-1}) simulated by **a** SLT **b** and SPT and **c** the observed climatology during June, July and August (from Xie and Arkin, 1996)

precipitable water between the NCEP-NCAR and DAO reanalysis datasets. While the tropically averaged precipitable water from the SLT simulation lies between the values estimated by the two observational datasets, the SPT simulation is less than either of the observed values.

The recent study by Gaffen et al. (1997) of precipitable water simulations in the AMIP results has also shown that there exists considerable variation in the simulation of precipitable water between models. They note that within the AMIP simulations there exists no relationship between the simulation of precipitable water and precipitation. In our simulations we find that SLT simulates both higher precipitation and precipitable water in the tropics.

Bates and Jackson (1997) have noted that lower values of precipitable water are found in the east Pacific vis-a-vis the western Pacific in most AMIP simulations. Tables 3 and 4 show the values for July and January for the two simulations and observations (NCEP/NCAR reanalysis). For our analysis we consider the eastern part of the ocean to be 120°E–150°E, 10°S–10°N, while the western part comprises the area bounded by 120°W–90°W, 10°S–10°N. We note that the precipitable water in the SPT run is underestimated (in comparison to the NCEP/NCAR reanalysis) while the precipitable water in SLT simulation is closer to the observed values.

The SLT simulation (Tables 3 and 4) has higher precipitable water in the west Pacific vis-a-vis the east Pacific while the SPT values for the east and the west Pacific are comparable. Later we shall show that this is related to differing response of the two schemes to SSTs especially at higher temperatures.

4.1 Relationship between SST and precipitable water

Figure 3 shows the variation of precipitable water (over the west Pacific region) and SST for the two simulations and for NCEP/NCAR reanalysis. We find that the SLT simulation of precipitable water during January (Fig. 3a) is larger than the SPT simulation. At lower temperatures it underestimates the precipitable water vis-a-vis the NCEP reanalysis and at higher SSTs the same is overestimated. In contrast, the SPT simulation consistently underestimates the precipitable water. During July (Fig. 3c), while at low SSTs SLT overestimates the precipitable water, it is in better agreement with NCEP reanalysis at higher temperatures (except at 302.5 K where it overestimates this quantity). The SPT simulation however underestimates precipitable water at all temperatures.

Bates and Jackson (1997) suggest that the varying precipitable water from the different AMIP models at the same SST indicates the influence of atmospheric dynamics on precipitable water. Comparing the wind patterns at 200 hPa during DJF (Fig. 5), we find that there are significant differences in the circulation patterns in the two simulations especially over the Indian, central Pacific and east Pacific regions. This strongly indicates that the modeling of moisture transport has a significant impact on the atmospheric dynamics (caused by latent heat release due to precipitation) and the amount of precipitable water (through convergence and divergence of moisture).

To further understand the role of dynamics we study the mean variation of specific humidity in the vertical as a function of SST. This vertical variation is strongly influenced by dynamics e.g., a region of descent will have a lower scale height of water vapor and hence lower precipitable water while ascent will cause the water vapor to be mixed more uniformly and thus increase the scale of height of water vapor (leading to higher precipitable water). In the tropics, Stephens (1990) suggests that specific humidity, q_l, at any level, p_l can be represented as:

$$q_l = q_0 \left(\frac{p_l}{p_0}\right)^{\lambda} \tag{1}$$

where q_0 is the near surface specific humidity and p_0 is the pressure at the surface.

Therefore the precipitable water w_p can be written as

$$w_p = \int_0^{p_0} q_l \, dp \tag{2}$$

Combining Eqs. (1) and (2) we can write the precipitable water as

$$w_p = \frac{q_0 p_0}{\lambda + 1} \quad . \tag{3}$$

The variation of λ (scale height index) as a function of SST for January and July are shown in Fig. 3b, d. From Eqs. (1) and (3) we can infer that for the same near-surface specific humidity q_0, a higher value of λ implies a rapid reduction in specific humidity in the vertical and thus a lower value of precipitable water (Fig. 3a, c).

Table 3 Table showing the precipitable water (kg m^{-2}) for January in east and west Pacific in the NCEP/NCAR reanalysis climatology (Climatology), and for the model simulations with SLT and SPT moisture schemes

Region	Climatology	SLT	SPT
West	45.8	48.5	35.9
East	38.5	37.3	35.2
Diff	7.3	11.2	0.7

Table 4 Table showing the precipitable water (kg m^{-2}) for July in east and west Pacific in the NCEP/NCAR reanalysis climatology (Climatology), and for the model simulations with SLT and SPT moisture schemes

Region	Observed (climatology)	SLT	SPT
West Pacific	44.4	44.7	37.2
East Pacific	39.1	37.3	35.2
Diff	5.3	3.2	2.0

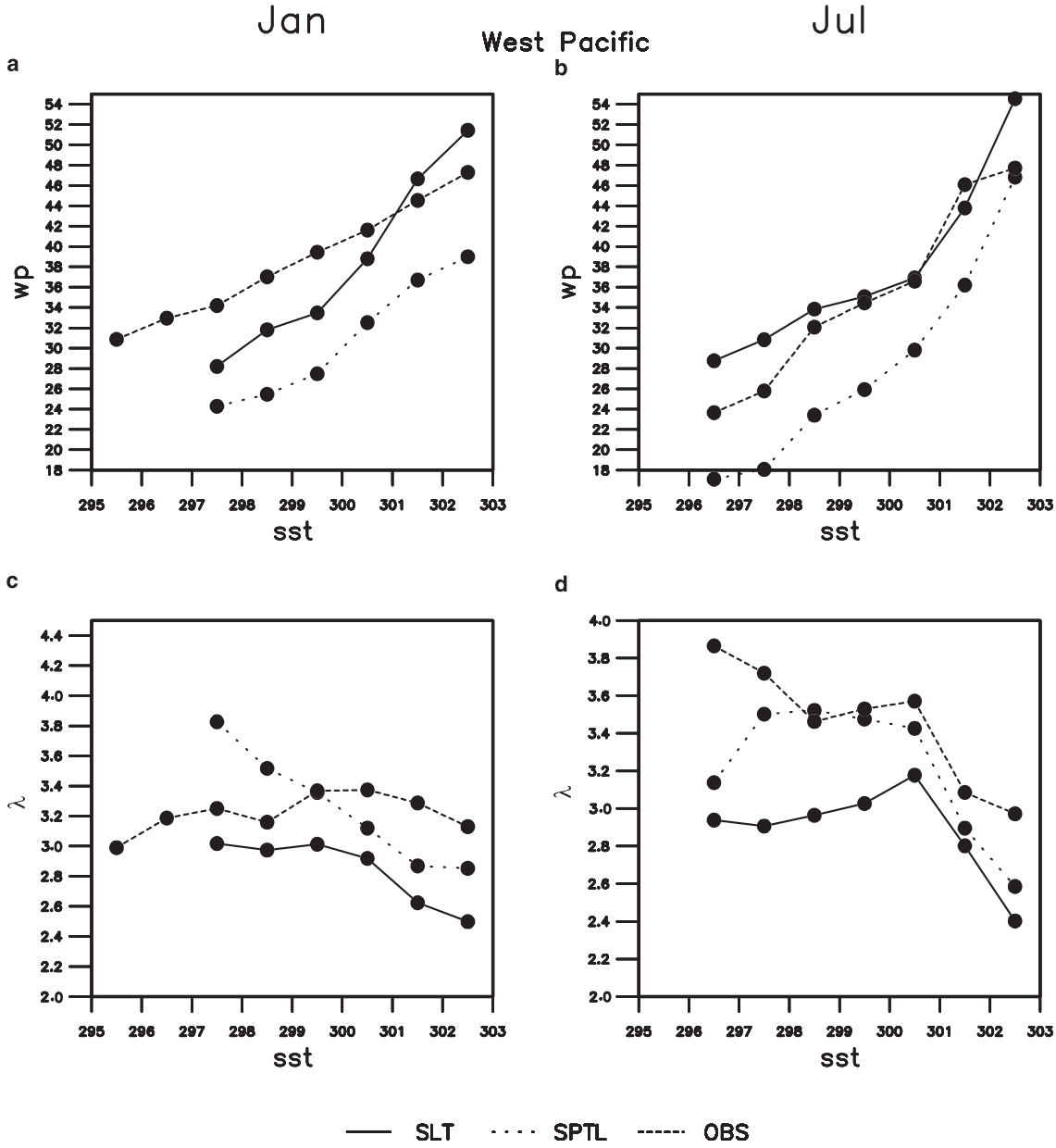

Fig. 3a–d Variation of precipitable water (wp) in kg m^{-2} and scale height index (λ) with SST for the SLT simulation SPT simulation and NCEP/NCAR reanalysis during **a,b** January and **c,d** July for the west Pacific region, dark full lines are for the SLT simulation. Dotted lines are for the SPT simulation, and dashed lines are for NCEP/NCAR reanalysis (obs)

We notice from Fig. 3b, d that the spectral simulation shows a larger value of λ vis-a-vis SLT simulations in the west Pacific region. Significantly the index λ is higher for the reanalysis data than the SLT simulation both in January and July. Qualitatively, both SPT and SLT simulations show a similar trend as the reanalysis data i.e., with increasing SST the scale height index reduces. However we should use λ values with caution as this is a derived quantity of two variables (in reanalysis) which have been strongly influenced by the model used i.e., precipitable water and specific humidity. Over most of the oceans, observations for near surface specific humidity are generally sparse and therefore these values might more strongly influenced by the values generated by the model. In the east Pacific, the response of both SLT and SPT models is very similar to that of the reanalysis for λ and w_p, though both underestimate λ in comparison to the NCEP reanalysis (Fig. 4).

Comparing the vertical profiles of specific humidity for January and July in the east and the west Pacific and the Indian Ocean (Fig. 6) we note that the profiles in the east Pacific are very similar for the SLT and SPT simulations in both months. However, the profiles are very different in the west Pacific with SLT having a higher water vapor content in the lower troposphere than the SPT simulation. Also we notice that this is most prominent in the lower levels of troposphere in January. This is related to λ (scale-height index) variation in the two

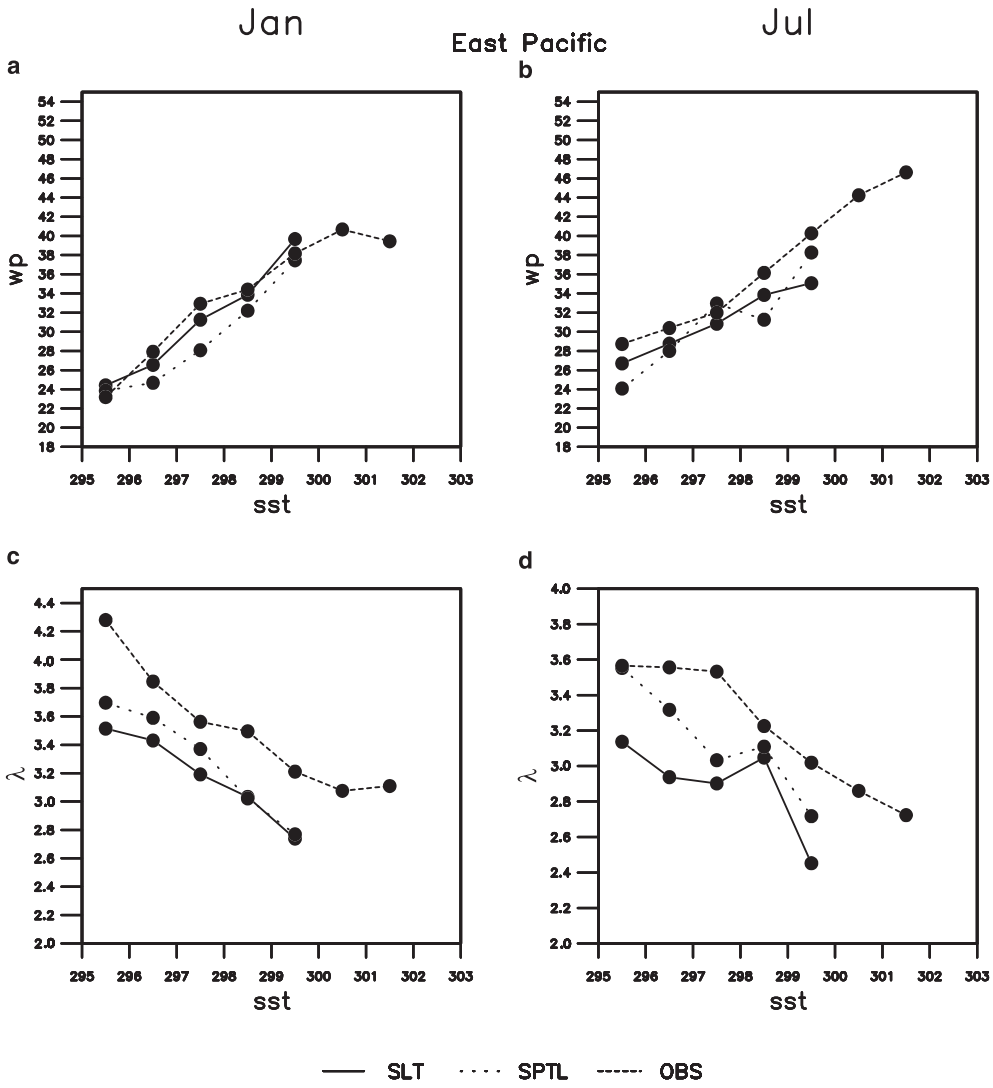

Fig. 4a–d Variation of precipitable water (wp) in kg m^{-2} and scale height index (λ) with SST for the SLT simulation SPT simulation and NCEP/NCAR reanalysis during **a,b** January and **c,d** July for the east Pacific region, dark full lines are for the SLT simulation. Dotted lines are for the SPT simulation, and dashed lines are for NCEP/NCAR reanalysis (obs)

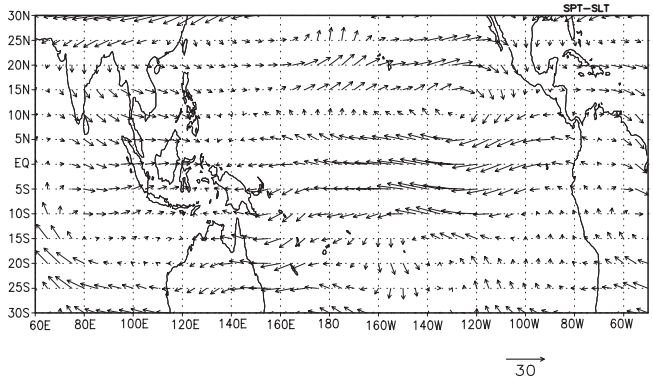

Fig. 5 Difference in 200 hPa winds during DJF between the SPT and SLT simulations

simulations. λ in the SPT simulation is higher (implying a smaller scale height) and this causes precipitable water to be smaller in the west Pacific. In the east Pacific where SSTs are lower, λ for both simulations are very close and the vertical profiles of specific humidity are also very similar. We notice a similar variation in the Indian Ocean region (80°E–90°E, 5°N–10°N). During winter when temperatures are lower, the profiles for this region are more similar than during the summer season. We find that in the lowest layers of the atmosphere both SLT and SPT simulations underestimate the specific humidity vis-a-vis the NCEP/NCAR reanalysis. Thus the combination of lower λ and lower near surface specific humidity causes the response of SLT model to SST for the simulation of precipitable water to be more realistic. The lower specific humidity in the lower levels could be related to the surface layer processes in the model and the interaction of surface processes with moisture advection needs to be studied separately.

4.2 Seasonal mean patterns of precipitable water

Comparing the precipitable water pattern during JJA and DJF seasons (Figs. 7 and 8) and the difference of

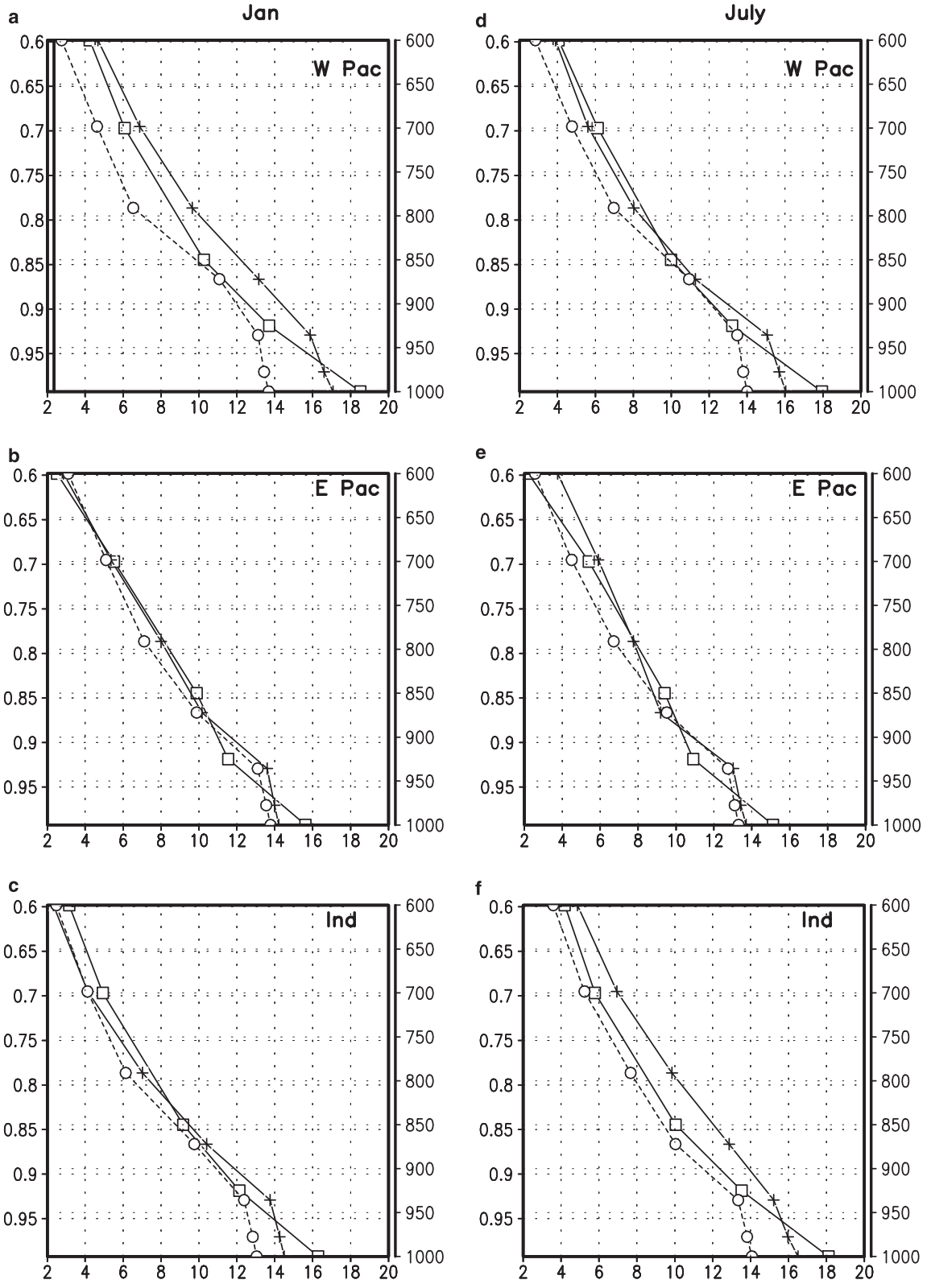

Fig. 6a–f Vertical variation of specific humidity (g/kg) during **a,b,c** January and **d,e,f** July in the east Pacific, west Pacific and Indian Ocean regions. ○ indicates the SPT simulation, Uindicates the NCEP/NCAR reanalysis, and + indicates the SLT simulations. The model profiles are plotted for the η vertical co-ordinates while reanalysis is plotted for mandatory pressure levels

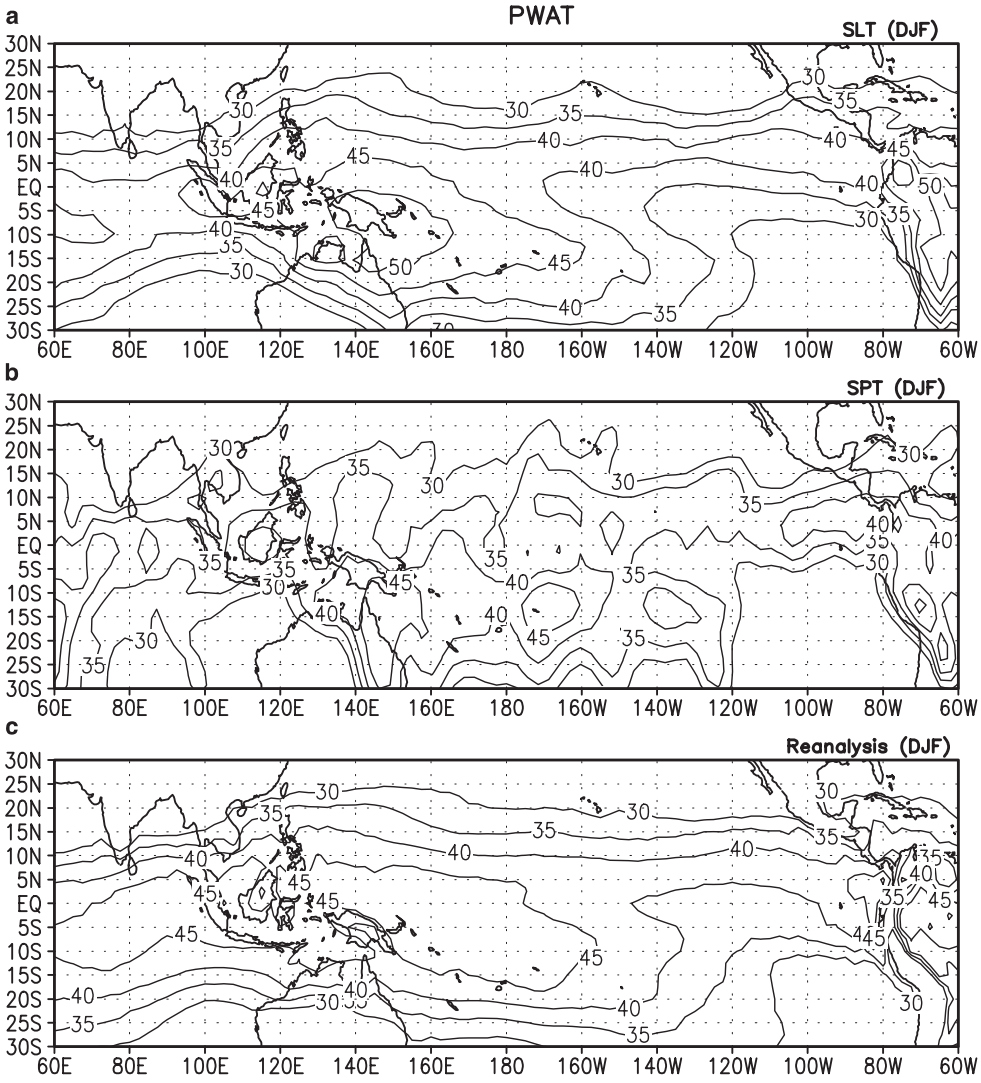

Fig. 7a–c Precipitable water (kg m^{-2}) for the **a** SLT simulation, **b** SPT simulation and **c** the observed climatology (NCEP/NCAR reanalysis) during DJF

precipitable water between the two simulations we note that regions of higher precipitation in the SLT (Fig. 1) simulation compare well with regions of higher precipitable water. Over the west Pacific region the precipitable water in the SLT simulation is much larger than in the SPT simulation and also in comparison to the NCEP reanalysis. Over the Indian region too, the SLT simulation shows larger precipitable water during the northern summer season. SLT's simulation over the Indian region during JJA compares well with NCEP/NCAR reanalysis while SPT underestimates the precipitable water in this region. As shown earlier, the specific humidity in the near-surface levels is much lower in both the models vis-a-vis reanalysis. However, the larger precipitable water in the SLT simulation could be related to greater specific humidity between 900–700 hPa levels in the west Pacific and Indian regions (Fig. 6).

4.3 Temporal variation of precipitable water

In Fig. 9 we show the temporal variation of precipitable water in the east and west Pacific in the two simulations. We note that in the SLT simulation the west Pacific precipitable water is always larger than in the east Pacific. However in the SPT simulation, the precipitable water is sometimes larger in the east Pacific also. We also note that the precipitable water in the west Pacific differs more in the two runs than the precipitable water in the east Pacific. This is related to the variation of scale height index λ (Fig. 3) which shows that the differences in λ and thus precipitable water is more prominent at higher SSTs. When studying the temporal variation of 500 hPa vertical velocity (Fig. 10) we find that the ascent over west Pacific in the SLT simulation is much stronger than in the SPT simulation, causing λ to be lower and precipitable water to be higher. We also find that ascent over the east Pacific is stronger in the SPT simulation than in the SLT simulation.

5 Impact of water vapor on vertical instability

Neelin and Held (1987) developed a simple model to understand the relationship between stability and organized

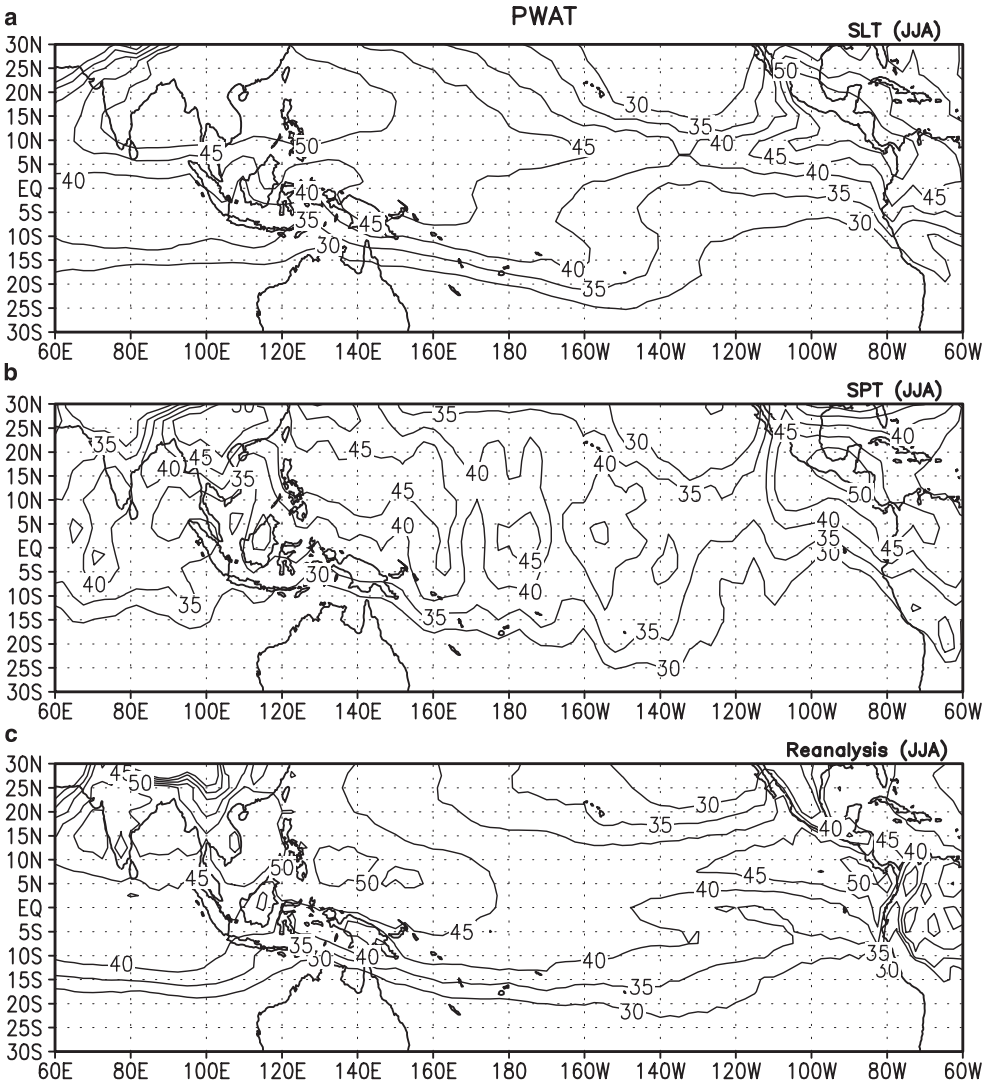

Fig. 8a–c Precipitable water (kg m^{-2}) for the **a** SLT simulation **b** SPT simulation and **c** the observed climatology (NCEP/NCAR reanalysis) during JJA

convection. Using this model Zhang (1994) has shown that differences in tropical precipitation between two simulations from a GCM can be related to the differences in vertical moist static stability (VMS). Using similar arguments, Nanjundiah and Srinivasan (1999) have studied the variation of precipitation in the Pacific basin.

Following Zhang (1994) we can write the relationship between VMS and precipitation P in the following way:

$$\frac{\Delta P}{P} \approx -\frac{\Delta m}{m} \tag{4}$$

Here $m = S + LQ$, the vertical moist stability (VMS) is given by the difference in moist static enthalpy between the upper and the lower layers of the atmosphere, S is the vertical dry static stability of the atmosphere (VDS), Q the difference between the amount of moisture in the upper and lower levels and L is latent heat of evaporation. Δm is the difference between VMS and ΔP, the precipitation difference between the two simulations.

From Eq. (4) and also from Fig. 12 we find that regions with $\Delta m < 0$ between SLT and SPT correspond closely to regions of higher precipitation in the SLT simulation (and vice-versa).

We can split the contribution to VMS into two parts

$$\Delta m = \Delta S + L\Delta Q \tag{5}$$

From Fig. 12 we find that ΔS (the difference in VDS) has little variation and does not contribute to the instability of the atmosphere in regions of high convection especially the Indian monsoon and west Pacific regions. However, $L\Delta Q$ (Fig. 12) and VMS (Fig. 11) have similar patterns of variation.

We notice that the vertical moist static stability of the spectral simulation is lower than that of the SLT simulation over the east Pacific, while SLT shows lower VMS in the western Pacific. In the west Pacific and over the Indian region, the VMS difference is caused by differences in precipitable water (and hence $L\Delta Q$, as moisture is mostly in the lower troposphere). Thus while the larger instability of west Pacific vis-a-vis the east Pacific in the SLT simulation is associated with higher convective activity over the west Pacific, the smaller differ-

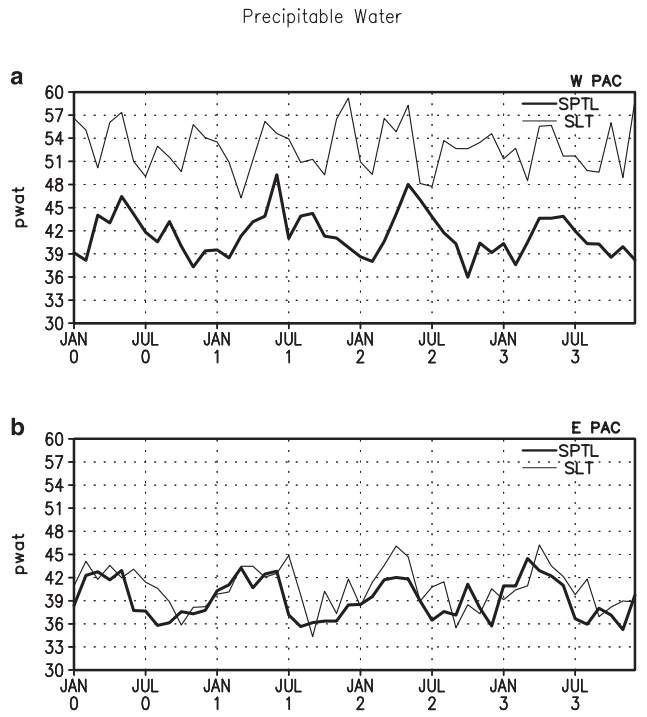

Fig. 9a,b Temporal variation of precipitable water (kg m^{-2}) in the SPT simulation (thick line) and SLT simulation (thin line) in **a** west Pacific (top) and **b** east Pacific (bottom)

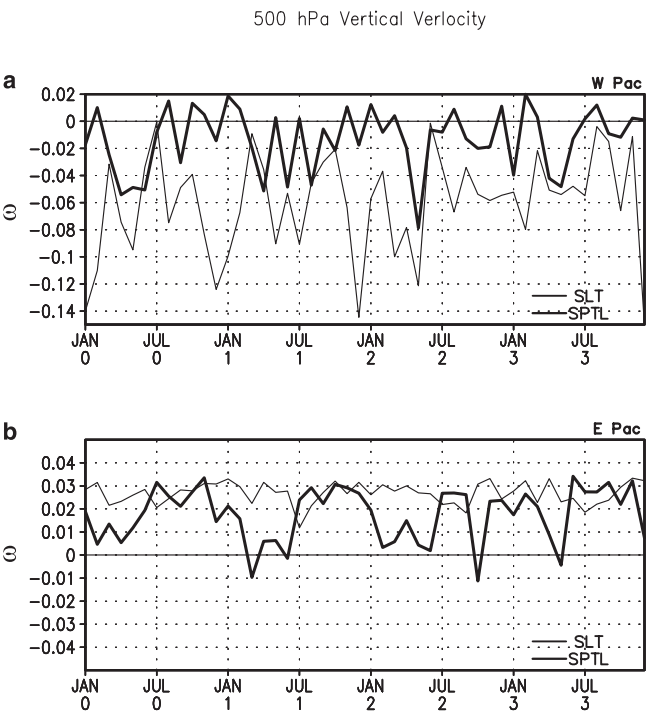

Fig. 10a,b Temporal variation of 500 hPa vertical velocity (10^5 * hpa sec^{-1}) in the SPT simulation (thick line) and SLT simulation (thin line) in **a** west Pacific (top) and **b** east Pacific (bottom)

ence in the VMS between the west and the east Pacific in the SPT simulation (due to increased stability as a consequence of smaller amounts of precipitable water) is associated with increased convective activity in the east Pacific.

5.1 VMS and the Indian monsoon

We now examine the vertical stability of the atmosphere and its relationship to precipitation differences in the Indian region. The differences of dry static stability VDS (S), VMS (m) and precipitation for JJA are shown in Fig. 13. It can be seen that the differences in precipitation closely correspond to differences in VMS but have little or no correspondence to differences in VDS. Regions where VMS in the SLT simulation is lower (i.e., the SLT's simulation is more moist statically unstable in comparison with the SPT simulation) closely correspond to the regions where rainfall in the SLT simulation is higher than in the SPT simulation.

5.2 Temporal variation of VMS

Comparing the time series of the VMS patterns in the east and the west Pacific (Fig. 14) in the two runs we note that in general, the difference VMS between the west and the east Pacific is larger in the SLT simulation than in the SPT simulation. This implies that while in the SLT simulation the east Pacific is much more stable than the west Pacific, the vertical stability of the two regions is almost same in the SPT simulation. Also comparing the VMS patterns in the two regions for the two simulations we note that the difference in VMS is larger in the west Pacific with SPT being more stable in this region than the SLT simulation. In the east Pacific, SPT is more unstable vis-a-vis the SLT simulation. In Fig. 15 we show the temporal variation of vertical dry static stability (VDS) in the east and west Pacific regions. We notice that in both these regions the SPT simulation has lower VDS, which implies that the atmosphere in this simulation is more dry statically unstable. Figure 9 shows that the precipitable water quantity is significantly larger over the west Pacific in the SLT simulation, while this quantity is of comparable magnitude over the east Pacific in both the simulations. The larger amount of precipitable water over the west Pacific causes the VMS in the SLT simulation to be lower over this region (through the $-L\Delta Q$ term in Eq. 5) associated with larger instability and greater convection.

6 Conclusion

The impact of moisture transport techniques on the seasonal mean simulation of tropical precipitation has been studied. We find that modifying the moisture transport from SLT to SPT has a significant impact on the seasonal mean precipitation in the tropics. The major significant differences are:

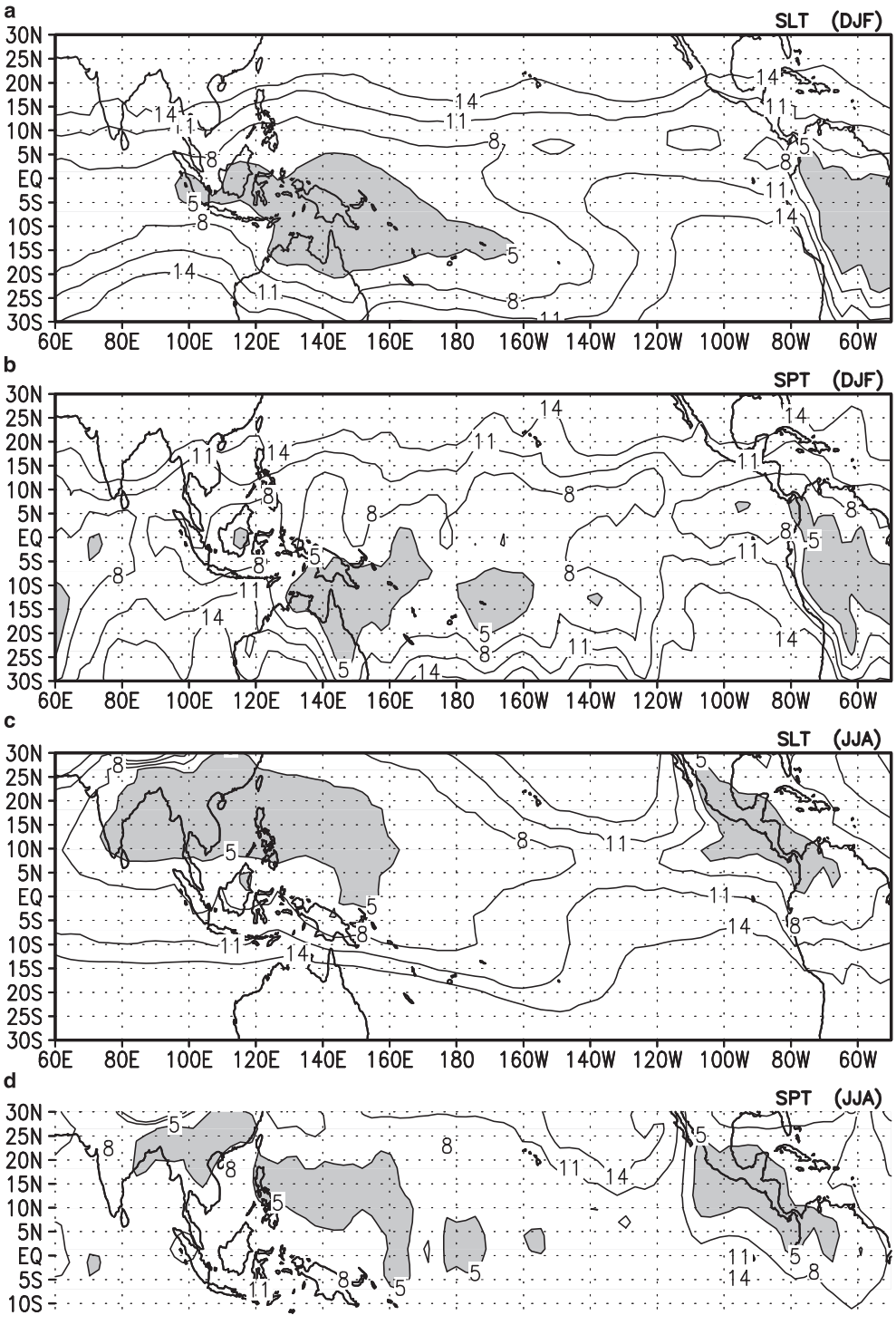

Fig. 11a–d Vertical moist static stability (VMS) for the SLT and SPT simulations for **a,b** DJF and **c,d** JJA (in kJ kg^{-1}). Regions with VMS below 5 kJ kg^{-1} are shaded

1. Decrease of rainfall over the Indian region during the monsoon (JJA) period
2. Decrease of rainfall over the west Pacific region
3. Increase of rainfall over the east Pacific

We also find that over most of the tropics the spectral method underestimates the total precipitable water in the atmosphere. This is due to differences in the vertical structure of water vapor in the SLT and SPT simulations. Using the Neelin and Held (1987) hypothesis we have shown that changes in precipitable water cause the vertical moist static stability (VMS) to be different. Over the west Pacific, SLT simulation shows a much larger value of precipitable water. This causes the VMS to be lower in the SLT simulation making this region more conducive for convective activity and higher precipitation. However, over the east Pacific, the precipitable water amount is similar in the two simulations. This

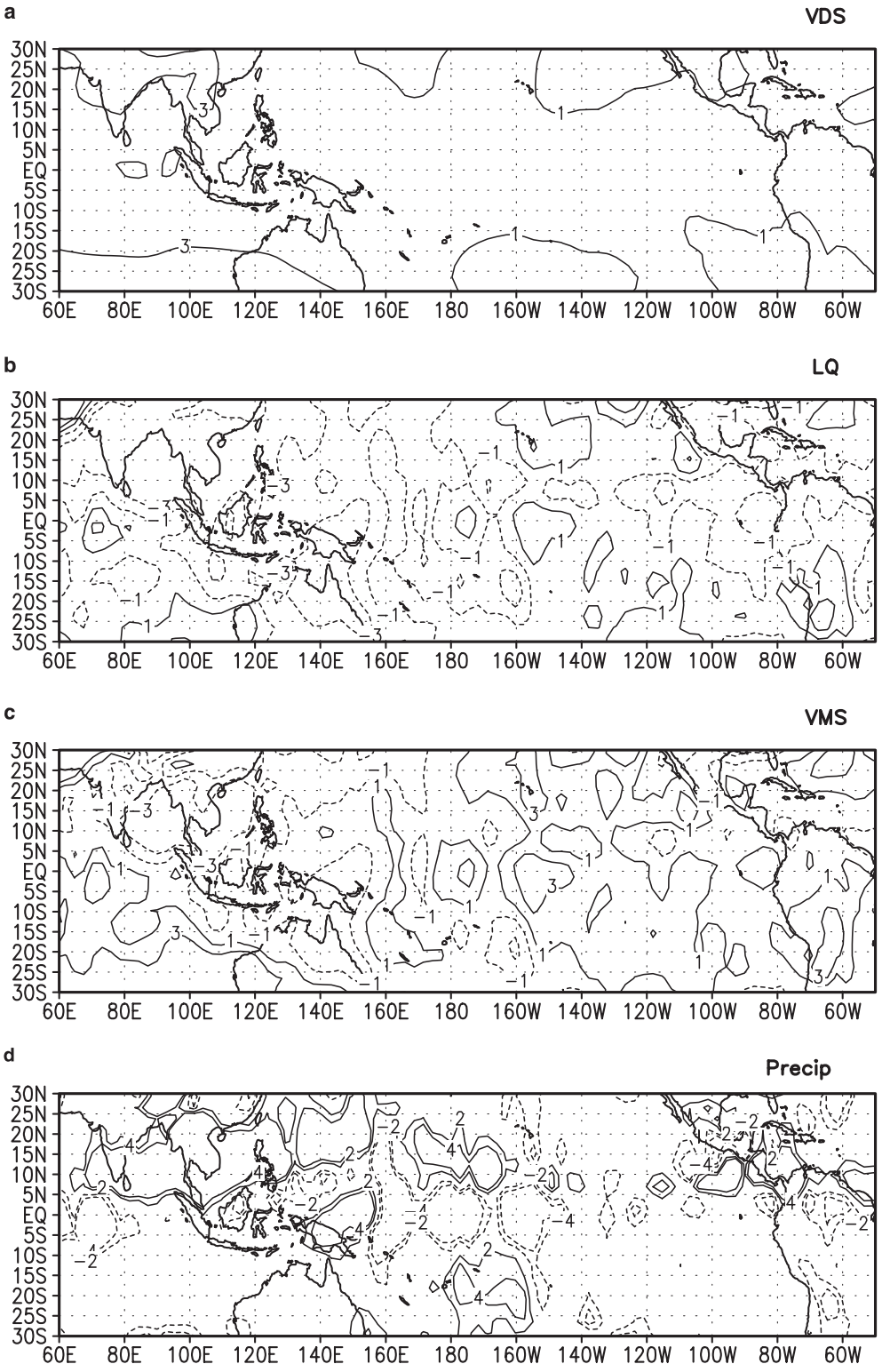

Fig. 12a–d Differences between the SLT and SPT simulations for **a** VDS (kJ kg^{-1}), **b** contribution of moisture to VMS (LQ, kJ^{-1}), **c** VMS (kJ kg^{-1}), and **d** precipitation (mm day^{-1}) during JJA

indicates that the response of the two models is very different at the higher SSTs found in the west Pacific while it is very similar over the relatively lower SSTs found in the east Pacific. These differences lead to higher precipitation over the east Pacific and lower precipitation in the west Pacific in the SPT simulation.

Similarly during JJA, we find that the precipitable water amount over the Indian region is lower in the SPT simulation (vis-a-vis the SLT simulation). Thus the SLT simulation has a more convectively unstable atmosphere with a more vigorous monsoon over this region. Thus, on the larger scale of the tropics and on the regional

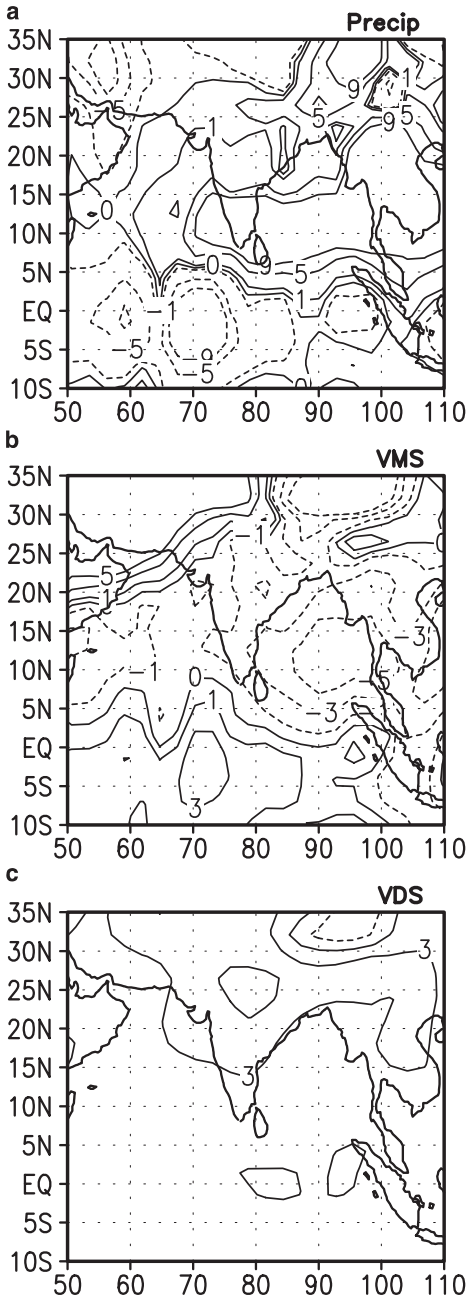

Fig. 13a–c Difference in **a** precipitation (mm day^{-1}) **b** VMS between the two simulations (kJ kg^{-1}) and **c** VDS (kJ kg^{-1}) between the SPT and SLT simulations over the Indian monsoon region during JJA

scale of the monsoons, modeling of moisture transport is seen to have a significant effect.

Acknowledgements The author thanks Profs J Srinivasan, Sulochana Gadgil and NV Joshi for their useful suggestions and detailed discussions. The author also thanks the Chairman of SERC-IISc for providing computational resources (especially on the IBM-SP2) for this work. The valuable and perceptive comments of the two anonymous reviewers, which helped in improving the paper substantially, are gratefully acknowledged. The parallel version of CCM2 used in this study was developed at Argonne and Oak Ridge National Laboratories under the US DoE CHAMMP Program.

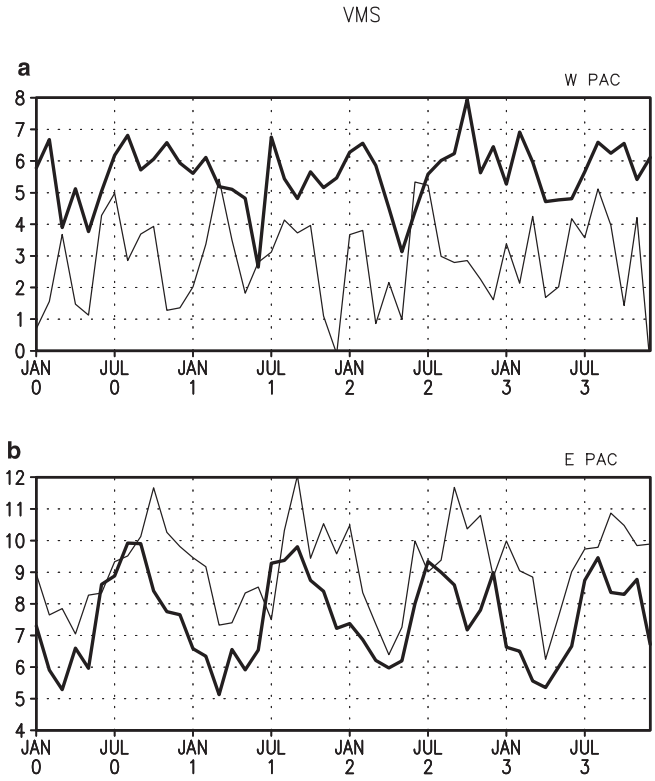

Fig. 14a,b Temporal variation of VMS (kJ kg^{-1}) in the SPT (thick line) and the SLT (thin line) simulation in **a** west Pacific and **b** east Pacific

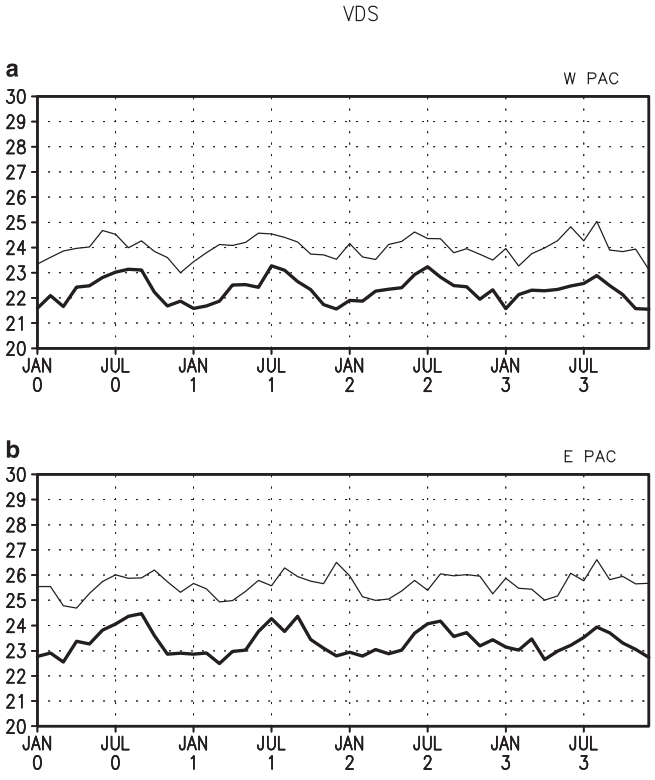

Fig. 15a,b Temporal variation of VDS (kJ kg^{-1}) in the SPT (thick line) and the SLT (thin line) simulation in **a** west Pacific and **b** east Pacific

References

Arpe K, Dumenil L, Giorgetta MA (1998) Variability of the Indian Monsoon in the ECHAM3 Model: sensitivity to sea surface temperature, soil moisture, and the stratospheric quasi-biennial oscillation. J Clim 11: 1838–1858

Bates JJ, Jackson DL (1997) A comparison of water vapour observation with AMIP I simulations. J Geophys Res 102: 21837–21851

Chen M, Bates JR (1996) A comparison of climate simulations from a semi-Lagrangian and an Eulerian GCM. J Clim 9: 1126–1148

Codron F, Sadourny R (1999) Saturation limiters for water vapor advection schemes: impact of orographic precipitation. Submitted

Gadgil S, Sajani S (1998) Monsoon precipitation in the AMIP runs. Clim Dyn 14: 659–689

Gaffen DJ, Rosen RD, Salstein DA (1997) Evaluation of tropospheric water vapour simulations from the Atmospheric Model Intercomparison Project. J Clim 10: 1648–1661

Hack JJ, Boville BA, Briegleb BP, Kiehl JT, Rasch PJ, Williamson DL (1993) Description of the NCAR Community Climate Model (CCM2). Tech Note, NCAR/T-382 + STR, pp 108 NCAR, Boulder, USA

Hastenrath S, Lamb PJ (1980) On the heat budget of hydrosphere and atmosphere in the Indian Ocean. J Phys Oceanogr 10: 694–708

Laprise R (1988) Representation of water vapour in a spectral GCM. In: Boer GJ (ed) Research activities in atmospheric and oceanic modeling. CAS/JSC Working Group on Numerical Experimentation, Rep 11: 3.18–3.21

Legates DR, Willmott CJ (1990) Mean seasonal and spatial variability in gauge-corrected, global precipitation. Int J Climatol 10: 111–127

Mo KC, Higgins RW (1996) Large-scale atmospheric moisture transport as evaluated in the NCEP/NCAR and the NASA/DAO reanalysis. J Clim 9: 1531–1545

Molod A, Helfand HM, Takacs LL (1996) The climatology of parameterized physical processes in the GEOS-1 GCM and their impact on the GEOS-1 data assimilation system. J Clim 9: 764–785

Nanjundiah RS, Srinivasan J (1999) Variations in precipitable water vapour and vertical stability during El Nino. Geophys Res Lett 26: 95–98

Neelin JD, Held IM (1987) Modeling tropical convergence based on the moist static energy budget. Mon Weather Rev 115: 3–12

Randel DL, Vonder Haar TH, Ringerrud MA, Stephens GL, Greenwald TJ, Combs CL (1996) A new global water vapor dataset. Bull Am Meteorol Soc 77: 1233–1246

Rasch PJ, Williamson DL (1991) The sensitivity of a general circulation model to moisture transport formulation. J Geophys Res 96: 13 123–13 137

Shea DJ, Trenberth KE, Reynolds RW (1990) A global monthly sea surface temperature climatology. NCAR Technical Note, NCAR/TN-345 + STR, Boulder, USA, pp 167

Sokal RR, Rohlf FJ (1981) Biometry: the principles and practices of statics in biological research. 2nd edn, Freeman WH, New York, pp 837

Stephens GL (1990) On the relationship between water vapour over the oceans and sea surface temperature. J Clim 3: 634–645

Williamson DL, Rasch PJ (1994) Water vapour transport in the NCAR CCM2. Tellus 46A: 34–51

Xie P, Arkin PA (1996) Analysis of global monthly precipitation using gauge observations, satellite estimates and numerical model predictions. J Clim 9: 840–858

Zhang GJ (1994) Effects of cumulus convection on the simulated monsoon circulation in a general circulation model. Mon Weather Rev 122: 2022–2038